Correlation effects in microwave observations of selected RS CVn-like stars

E. Budding[a,b,*], J. Lim[c], O.B. Slee[d], S.M. White[e]

[a]*Central Institute of Technology, P.O. Box 40740, Wellington, New Zealand*
[b]*Carter Observatory, P.O. Box 2909, Wellington, New Zealand*
[c]*Academia Sinica Inst. of Astronomy and Astrophysics, PO Box 1-87, Nankang, Taipei 11529, Taiwan*
[d]*Australia Telescope National Facility, Vimiera and Pembroke Rds., Marsfield 2121, NSW, Australia*
[e]*Department of Astronomy, University of Maryland, College Park, MD 20742, USA*

Abstract

Sets of dual frequency microwave data on selected chromospherically active stars, from the Australia Telescope Compact Array, have been investigated for their auto and cross-correlation effects. Comparison of cross-correlation peak values with theoretical expectation indicates a high degree of real physical connection between the emission at the pairs of frequencies (4.8 and 8.64 GHz) compared. This fact should help constrain models for the emission mechanism.

The timescale of observed time-shifts between the emissions at the two frequencies is consistent, in general, with the underlying energization being propagated by magnetohydrodynamic waves in a compact turbulent medium. © 2002 Elsevier Science B.V. All rights reserved.

1. Introduction

RS CVn-like stars were originally recognized by optical 'wave distortion' effects associated with very large 'starspots' (Hall, 1976). Prototype RS CVns are binary systems, consisting of a late F or early G type dwarf and a late G to K type subgiant. 'Chromos-pheric' spectroscopic emissions and other characteristics of RS CVns, and similar 'active' stars, point to large surface effects, basically resembling those of the Sun, but enhanced by one or two orders of magnitude in scale. The idea of greatly scaled up solar active regions is also supported by microwave emission tending to anticorrelate with broad-band optical flux (Budding et al., 1999; Slee et al., 1986).

Previous authors have subdivided microwave emission from active stars into a shorter-term (minutes to hours) impulsive component, associated with giant flares, and the quiescent component that undu-

*Corresponding author.
E-mail addresses: Edwin.Budding@cit.ac.nz (E. Budding), jlim@asiaa.sinica.edu.tw (J. Lim), bslee@atnf.csiro.au (O.B. Slee), white@astro.umd.edu (S.M. White).
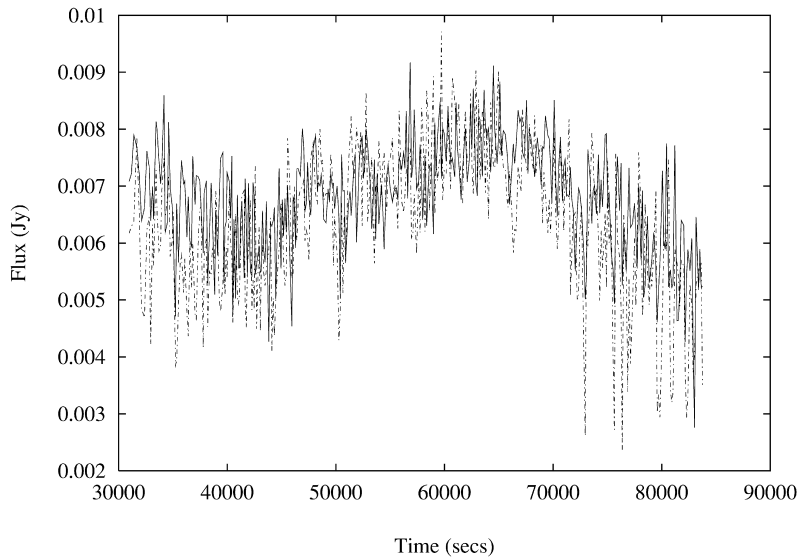
Fig. 1. Plot of high time resolution (3 min) observations of V824 Arae as observed on 3/5/96. The C (full) and X-band (dot–dash) data-sets are superposed.

lates over a timescale comparable to the stellar rotation period (Lim et al., 1992; cf. also, e.g., Doiron and Mutel, 1984; Patterson et al., 1993; Slee et al., 1986). These latter were associated with the large 'halo' formations resolved by VLBI observations (cf. Lestrade et al., 1986; Mutel et al., 1986; Slee et al., 1987). This classification scheme is not always clear in individual data-sets, while more recent authors (cf., e.g., Gagné et al., 1999; Güdel, 1997; Jones et al., 1996) have argued for flares, or multi-flaring, as the basic electron energization process.

A multi-wavelength campaign on the RS CVn binary CF Tucanae in 1996 (Budding et al., 1999) included microwave data, gathered with the Australia Telescope Compact Array[1] (ATCA). Fluctuations at the relatively quiescent level of 1–2 mJy, observed at 4.8 and 8.64 GHz, led to studies of their auto- and cross-correlation properties. Fig. 1 shows high-time resolution observations of V824 Arae as observed on 3/5/96. The trend of overlap of the C (4–5 GHz) and X-band (~8 GHz) data is again quite clear, suggesting further application of correlation analysis

to this and comparable data-sets. Hence, in this paper we seek to examine such correlation effects for comparable active stars, where sufficient microwave data exist. Besides CF Tucanae, we consider data-sets for the stars V824 Arae, HR 1099, AB Doradus and AU Microscopii.

2. Correlation effects

The auto-correlation function, which contains information about the predominating timescales of changes in flux density, is formed by summing the products of ordinates linearly interpolated to uniform time spacing. This symmetric function (cf. Fig. 2) shows, apart from the central narrow peak corresponding to a single bin-width, generally a broad half-width for the 4.80 and 8.64 GHz data-sets, reflecting the rather long timescale of change for a signal undulation, compared with available time resolutions.

The cross-correlation, showing the temporal relationship between flux density changes at the C (in this case, 4.80 GHz) and X-bands (8.64 GHz), is also presented in Fig. 2. This particular data-set corresponds to about 3 h after ~22h15 on 1/5/96, during a period of good signal strength (~12 mJy). Here the
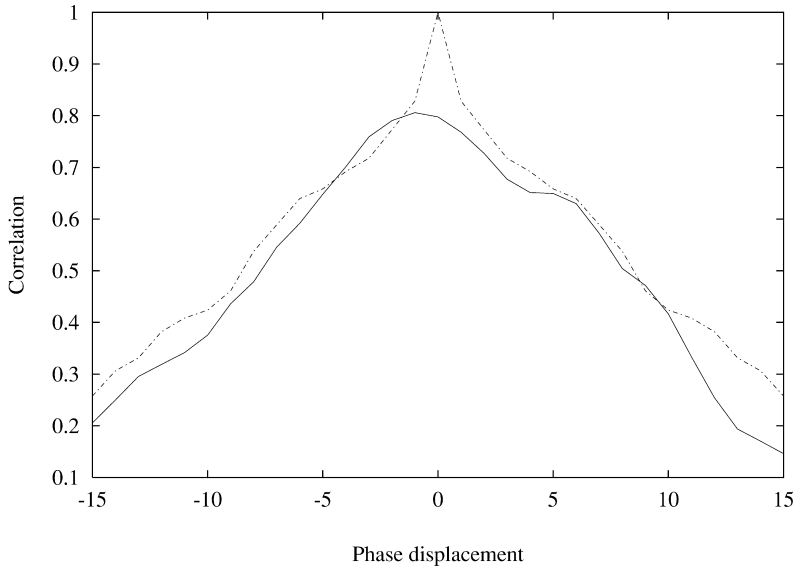
Fig. 2. Correlation functions for about 170 min of J. Lim's V824 Arae data, observed after ~22h15 on 1/5/96, represented by points evenly spaced at intervals of 100 s. The (dot-dashed) auto-correlation of the 4.80 GHz data is shown together with the asymmetric cross-correlation of 4.80 and 8.64 GHz data (continuous).

8.64 GHz light curve was fixed (the usual arrangement) and the 4.80 GHz data shifted in time at intervals of 100 s. The cross-correlation shows a noticeable asymmetry such that the curve's peak is shifted to negative lags. This means that the best agreement between the two data-sets happens when the intensity values from the 8.64 GHz data-set are multiplied with those at 4.80 GHz occurring a few minutes *earlier* in time. This particular data-set is then atypical: usually we have found that the lower frequency data effects tend to be somewhat delayed with respect to those at the higher frequency.

Other subsections of the light curves show comparable results, although a C to X-band shift is sometimes not so well defined, for example towards the end of the V824 Arae 3/5/96 data-set (Fig. 1). This could be expected from the irregularities in this low S/N raw data, particularly for the X-band, late in the data-set, as can be seen in Fig. 1.

The appropriate choice of interval and time resolution has been approached on a quasi-experimental basis. In order to expect significant correlation effects it would be reasonable to set the interval of interest sufficiently large so as to include clearly discernible trends in the data. For example, there is a

minor peak in the data shown in Fig. 1 between around 44 000 and 50 000 s, although this is hardly bigger than the noise level at 1 min integration. Since the timescale of the effect is about 6000 s, representative S/N values, which strongly affect the results as will be shown later, could be significantly improved by integrating to 10 min. There would still be 10 data points in the interval of interest, with the S/N effective for this feature increased by a factor of ~3.

2.1. Methodology check

The effects of real displacements and noise between one data-set and another was tested by taking an initial reference data-set and introducing a controllable level of noise to it. This was carried out by using the random number generator *RAN2*, as given by Press et al. (1988). This produces numbers x_i distributed uniformly on the range $0 \le x_i \le 1$. These can be related to values of the standard normal variate z_i, whose probability function $P(z) = \frac{1}{2} \, \mathrm{erf}(z^2/2)$ can be taken to correspond to $x_i - 0.5$, i.e. $z_i = P^{-1}(x_i - 0.5)$, for $0.5 \le x_i \le 1.0$. For $0 \le x_i < 0.5$ we can write $z_i = -P^{-1}(0.5 - x_i)$. Individual ordinates

y_i, when perturbed by normally distributed noise of s.d. σ, are then obtained as $y_i + \sigma z_i$. Additionally, a given time-shift was added to all the data-points of this comparison set, and the cross-correlation between it and the original reference data examined.

The results of this experiment are shown in Fig. 3. We remark on the following salient features of these results: (i) the peak of the cross-correlation survives the introduction of a relatively large noise level; (ii) the cross-correlation peak faithfully reflects the given time-shift, and is quite robust against the level of introduced noise.

Regarding point (i), we can consider the decline Δf_1 from the maximum of the auto-correlation experienced by the cross-correlation f_c, as a result of noise σ in the comparison data set, from the form

$$f_{c\max} = \frac{\Sigma[y_i(y_i + \sigma z_i)]}{(\Sigma y_i^2 \Sigma(y_i + \sigma z_i)^2)^{1/2}}. \tag{1}$$

With a little manipulation, we then find

$$\Delta f_1 = \sigma^2/2\overline{y^2}, \tag{2}$$

where $\overline{y^2}$ is the mean square value of the flux densities, and $\sigma^2/2\overline{y^2}$ is small compared to unity. In fact, $\sigma^2/2\overline{y^2}$ would be of order $1/2(S/N)^2$ for signals

S that are physically connected and not rescaled, as in the present trials. If the correlations are calculated by first subtracting ordinates from their mean values, so as to take out the effects of arbitrary scaling from one data set to another, then the decrement in (2) is scaled up by $\overline{y^2}/y_2^2$, where y_2^2 represents the real signal variance in the original data set. This foregoing result should allow us to examine the extent of real physical connection between separate data-sets in the presence of a specified amount of noise N, and, if such a direct connection exists, constrain underlying physical models.

In Fig. 3 we verify that the decline from the cross-correlation peak with increasing noise σ is directly proportional to σ^2, as given by the foregoing expression. The highest maximum (when $\sigma = 0$) is somewhat less than the unity autocorrelation peak, due to a slight loss of numerical identity associated with interpolation of the ordinates to phase-shifted values.

Concerning point (ii); the lateral shift Δx_m of the cross-correlation peak can be estimated on the basis of a parabolic fitting to the three points nearest to the maximum. These points have co-ordinates $(x_1 - s)$, f_1; x_1, f_2; $(x_1 + s)$, f_3, say. Then the abscissal location of the peak x_m is given by
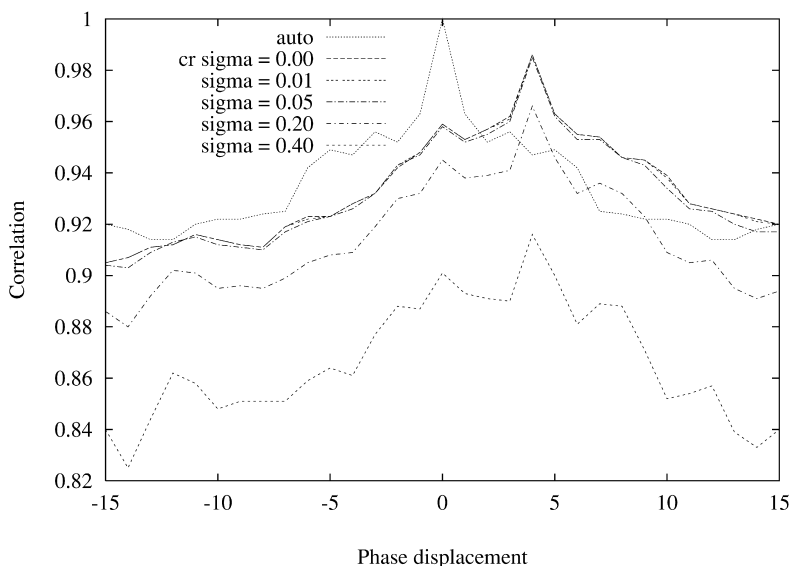

Fig. 3. C-band data from CF Tucanae observations (cf. Table 1) was correlated with a time-shifted copy of itself, to which a controlled amount of noise was added.

$$x_m = x_1 + (f_1 - f_3)s/2[(f_1 + f_3 - 2f_2)]. \qquad (3)$$

Taking the separation of abscissal reference points s to be the reciprocal of the number of points in the data-set $1/n$, we will find a shift of the order of

$$\Delta x_m = 2\Delta f_1/n, \qquad (4)$$

due to the effect of random noise in the data.

In Fig. 3 it can be seen that the asymmetry of the cross-correlation peak does increase slightly with increasing noise, but the perturbation is hardly significant even when S/N declines to ~3. This implies that shifts of the cross-correlation maximum can be effective in measuring a real time delay between physically correlated data-sets even for relatively low S/N data. For example, for a set of physically co-incident signals at two frequencies, for which the S/N value was 10, say, (typical, for the current data-sets) the effect of the random noise in disturbing the peak of the cross-correlation from zero would be ~$1/(S/N)^2 = 1\%$ of one phase step, if the correlating is done directly on the flux densities.

It is interesting, in this context, to note the studies of cross-correlations of transcontinental 408 MHz observations of interstellar scintillation in pulsars (Slee et al., 1974). The degradation of the cross-correlation maximum considered by Slee et al. (1974) arising from the effects of white noise in the signal is essentially similar to formula (1) above. Analysis of the relative shift between the auto- and cross-correlation curves allowed a determination of scintillation pattern drift velocities between the two spaced receivers.

3. Data

Table 1 collects the information on the data-sets analysed. There were originally 23 of these, but careful checks of data quality have reduced these to the 13 for which results are shown in Table 1.

The first three sources are standard RS CVn binaries and their identifications in the *Catalog of Active Binary Stars* (Strassmeier et al., 1993) are

Table 1
Stellar data sample

Star name & ident.	Observation date	Total obs. time min. C/X	Interpol. int'val min. C/X	Range of flux density C mJy	Range of flux density X mJy	Auto-corr. $1/e$ width min.	Cross-correlation Peak C/X	Cross-correlation Offset min. C/X	Rem.
V824 Arae	3/11/93	956	68.27	1.5–5.2	0.5–5.1	130±15	0.95	25±7	(a)
CABS 141	1/5/96	919	22.42	0.5–12.4	0.5–13.0	136±12	0.98	10±1	
	2/5/96	804	22.33	2.5–6.6	2.7–8.5	111±20	0.82	–9±2	(b)
	3/5/96	876	12.00	4.9–8.4	4.5–8.1	81±22	0.82	28±4	(c)
CF Tucanae CABS 8	26–28/6/98	4211	60.16	0.7–2.0	0.5–1.7	191±8	0.80	–35±4	(d)
HR 1099 CABS 29	14/9/93	516	34.40	298–325	325–354	99±13	0.92	–16±4	
	23/8/94	458	35.23	44–50	38–48	35±9	0.72	15±12	
	24/8/94	454	34.92	47–53	37–42	88±28	0.74	62±5	(e)
AB Doradus HD 36705	15/11/94	960	34.29	1.5–7.4	1.5–6.7	72±3	0.98	4±2	(f)
	16/11/94	993	34.24	1.6–5.3	2.0–5.4	40±4	0.84	4±3	
	14/10/97	560	4.00	1.8–8.9	1.2–8.1	54±7	0.82	0±1	
	15/10/97	804	4.00	1.3–7.0	1.2–5.2	60±5	0.75	6.5±0.5	
AU Microscopii Gliese 803	6/9/98	264	12.00	0.2–1.5	0.2–1.8	24±1	0.66	11±1	

Remarks: (a) Cross-corr. is asymmetric, such that a longer time-shift interval will tend to give a longer C–X lag. (b) Coarse time resolution over a wide data interval. (c) A number of different time intervals and resolutions tried for this data set. The results quoted are representative for most of the data. (d) These results were discussed in Budding et al. (1999). Note sign of the shift. (e) The high cross-correlation peak for this data is consistent with the very high S/N for HR 1099 data, but the time lag is remarkably long. (f) The higher time resolution data show more structure in the correlation curves, but all the AB Doradus curves have high cross-correlation maxima with relatively small displacements.

included. The fourth example is the well-known, rapidly rotating, cool dwarf AB Doradus, which shares many of the basic characteristics of the classical RS CVn stars. The fifth example is the well-known flare star AU Microscopii, which shares some of the physical characteristics of AB Doradus although it rotates less rapidly.

4. Analysis and results

Different approaches were taken in evaluating the listed correlation results from the given data samples, though some procedures were common to all analyses. Thus, data were first cleared of any obviously spurious points and then linearly interpolated to a constant time interval. This was done in order to minimise the effect of short calibration breaks, and, in the case of AB Doradus, the presence of short, impulsive flares. It was not possible to maintain the same interpolation interval for all data sets, however. On some nights L (~1.4 GHz) and S (2–3 GHz) and C and X-band recording were interspersed at 30 min intervals, while on other nights the stellar signal had to be integrated for hourly intervals to achieve an acceptable S/N ratio. This is reflected in the entries in column 4 in Table 1. We chose to retain only C and X-band data for detailed analysis. The highest time resolution used (4.00 min) was that for AB Doradus in October 1997, when a $S/N = 10$ was obtained, with recording exclusively in the C and X-bands.

Correlations (both auto and cross) were first performed by shifting one data-set with respect to the other, by times (δT) set to integer multiples of the interpolation interval (i.e., the sampling interval of the interpolated data set), and computing the linear correlation coefficient at each shift. The relative shifts were done in one direction, up to a maximum of 10% of the total number of integrations in the sets, and then for the cross-correlation the direction of shift was reversed to obtain the complementary set of values. The correlation coefficients were then plotted and fitted with gaussians. This yielded the axis of symmetry and $1/e$ width and their errors. The values listed in Table 1 are the average of the auto-correlation $1/e$ widths for C and X-bands.

This method of computing the correlations suffers

from the disadvantage that the number of values used in the computation drops as the shift δT grows larger due to the finite length of the data sets. On the other hand, one does not need to assume that the missing 10% of data has any particular periodicity, other than its temporal scale is similar to that of the whole data-set.

In an alternative procedure the observation interval of interest ΔT is extended by extra intervals added to the beginning and end of the observed data, of extent equal to the range over which the correlation functions are to be sampled. This is carried out by appending data from the beginning of the range ΔT to the end, and prepending data from the end of this range to the beginning of ΔT. The two ΔT endpoint data values are set to their average, and there results a quasi-periodicity about the interval of interest. If the object were a binary then its orbital period could be used as the ΔT chosen for the analysis, and a real quasi-periodicity of the flux densities with this period could be feasible.

While both of these approaches have difficulties of interpretation away from the ordinate axis ($\delta T = 0$) of the correlation diagrams, they generally concur for $\delta T \lesssim \Delta T/2$ (for the same intervals and bin-sizes). In practice, the sidewindows were never taken to be larger than about 10% of the interval. The outputs of the two approaches were compared, and generally found to be in close agreement. Average values have been listed in columns 7 and 8 of Table 1. We note that the median time displacement found here (irrespective of the sense of the displacement) depends markedly on the stellar type. For the RS CVn-like binaries the median is 20.5 min.; for the single smaller stars (AB Doradus and AU Microscopii) the median C/X displacement is only 4 min.

Some typical outputs from the correlation analyses of all five stars studied are shown in Figs. 4–8.

5. Discussion

Budding et al. (1999) discussed the microwave correlation effects they examined for CF Tucanae in terms of an emitting medium scanned at different effective depths by observations of different frequencies. Their model placed $\tau = 1$ surfaces in X and C-bands at around 0.47 and 0.57 $R_\odot$ above the
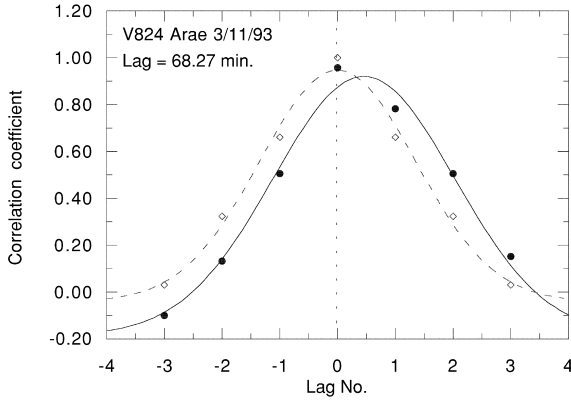
Fig. 4. Correlation curves for the 3/11/93 data on V824 Arae. The calculated values of the correlation functions (auto = open diamonds, cross = full circles), in this and the following diagrams, have been fitted here with gaussians. The axial shifts of such functions were used to estimate the lags or leads listed in Table 1.

active K-type subgiant's photosphere. An explanation for time-shift in the maximum of the cross-correlation was sought in terms of magneto-hydrodynamic wave propagation through this star's corona. The present paper appears to support this in a general way, although the picture is not as straightforward as Budding et al. (1999) suggested.

Whilst we may consider one source of energization propagating as a wave through the active stellar corona, the medium is probably locally highly irregular, having condensations with their own peculiar velocities in the vicinity of the $\tau = 1$ surfaces. Moreover, we cannot be certain at what height in the
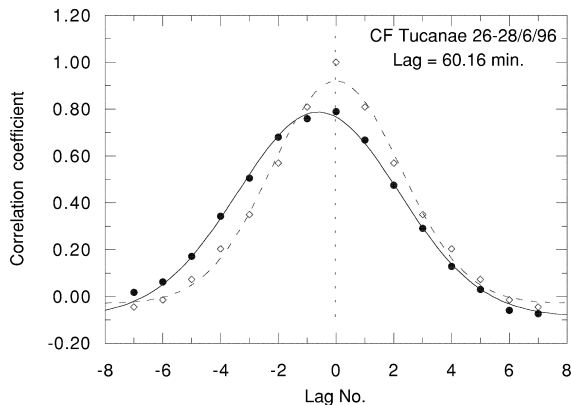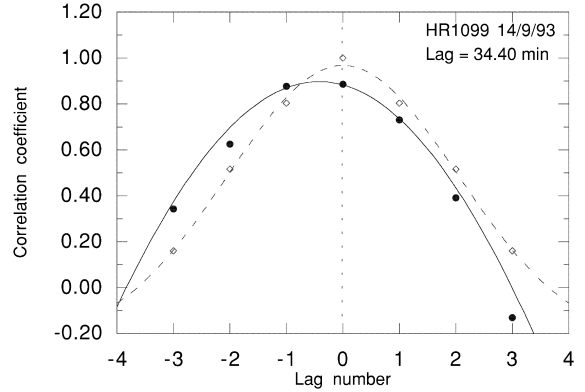

Fig. 6. Correlation curves for the first of the HR 1099 data sets.
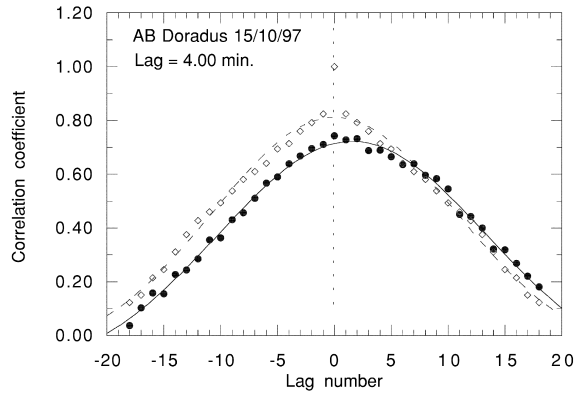
Fig. 7. Correlation curves for AB Doradus.

Fig. 5. Correlation curves for CF Tucanae (cf. Budding et al., 1999).
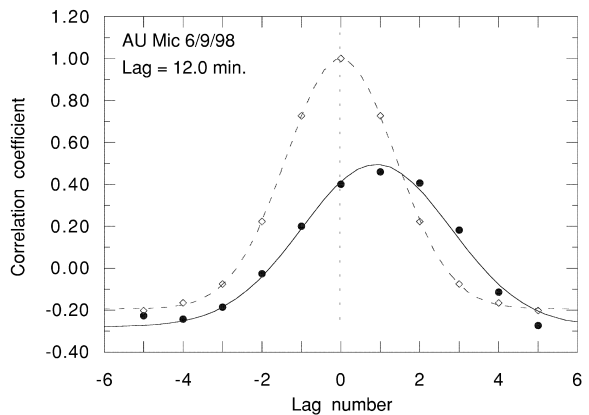

Fig. 8. Correlation curves for the flare star AU Microscopii.

corona an energy source, which may dominate the emission regime for some period of time, may originate. In this situation, we could expect measured lag or lead effects to trend towards a particular scale of time separation $\langle \Delta t \rangle$, depending on the mean separation of the emitting layers Δs_{C-X} and the energization wave velocity v_{MHD} in an unperturbed medium, i.e. $\langle \Delta t \rangle \approx \Delta s_{C-X}/v_{MHD}$. Individual values would, however, be perturbed from such an idealized situation.

The median value for RS CVn-like binaries determined from the Table 1 data-sets is in keeping with this scenario. We would then note the implication, as a consequence of the results, of a rather denser, and generally more extended coronal microwave emission region in these active stars than corresponds to the Sun, certainly in its quiescent phase. The corresponding $\tau = 1$ surfaces are there only around 10% (at most) of the deduced separations of these surfaces in the active regions of RS CVn stars. However, the dwarf single active stars AB Doradus and AU Microscopii appear to show different properties. The short separations for the C and X emitting layers for these stars would suggest size scales more like those of the Sun.

Alternative explanations of the measured lags are also possible. Radio flares on active stars are often modelled as expanding plasmoids, in which nonthermal electrons are trapped on magnetic field lines in a source expanding outwards from the stellar surface. As the source expands, its magnetic field strength necessarily drops and the electron energy distributions also evolve. This model finds support in VLBI observations that show apparent increases in source size with time (Mutel et al., 1998; Trigilio et al., 1993) and apparent motion of sources (Lebach et al., 1999). In this model, as in the similar 'fireball' model for the radio emission of γ-ray bursts (e.g., Waxman et al., 1998), one expects radio emission to peak initially at high frequencies. With the source evolution, the location of the peak in the radio spectrum will decrease in frequency, and this can produce an apparent delay in the lower frequency emission relative to higher frequencies. In this model, the expansion speed can again be assumed to be of the order of the Alfvén speed. However, such a model would not directly explain those few cases where the lower-frequency emission precedes the higher frequency.

Another possible factor which would influence the correlations measured here is beaming of the radio emission. Lim et al. (1994) argued that beaming was observed from AB Doradus because it was the most plausible explanation for the narrow width of peaks in the rotationally-modulated light curve, and there was some evidence that the 4 GHz beaming pattern was wider than the 8 GHz beaming pattern. However, this effect has not been seen on any other star, and so we believe that it is unlikely to explain the overall pattern of our results.

6. Conclusions

Our main findings can be presented as follows:

(i) The properties of the correlation functions for microwave data at a given pair of frequencies (usually X and C-band, i.e., 4–5 GHz and 8 GHz), considered previously by Budding et al. (1999) for CF Tucanae, are found to be generally similar to those of corresponding correlation functions for some similar active RS CVn stars.

(ii) The value of the cross-correlation maxima obtained for the pairs of microwave data-sets studied is consistent with the flux densities being of essentially the same origin, i.e. the pattern of variations observed at the two wavelength regions is probably inherently the same, but perturbed by random noise at the two frequencies, to an extent predictable from the known S/N ratio. This fact should introduce some constraint on physical models of the emission.

(iii) Systematic lags and leads, of the order of minutes, between one data-set and the other are observed at the two frequencies studied, but these vary appreciably in magnitude and even direction (e.g. Budding et al.'s (1999) shift for the CF Tucanae data was, in fact, negative).

(iv) The median value of observed time-shifts of the data sets Δt between pairs of microwave frequencies is of the same order as the propagation time for magnetohydrodynamic waves between coronal layers that can be reasonably associated with the predominating source locations, i.e. $\langle \Delta t \rangle \approx \Delta s_{C-X}/v_{MHD}$. This would correspond with the model considered by Budding et al. (1999). Differences in individual time-shifts may be associated with the effects of turbulence in the source medium.

(v) The X to C-band time-shifts for AB Doradus

are noticeably shorter than those obtained for the classical RS CVn binaries. This is in general keeping with the larger scale structures one might expect for the subgiant containing binaries – generally by one order of magnitude – as distinct from the conditions near a rapidly rotating single cool dwarf. However, the single result for the more slowly rotating dwarf AU Microscopii is appreciably longer than those for AB Doradus.

(vi) It would be desirable to continue to study these effects for active stars with microwave flux density measurements which are (a) more extensive in time; (b) having inherently higher S/N values and (c) distributed over a range of microwave frequencies; as well as testing the underlying scenario against more general multi-wavelength data (including optical and other wavelengths).

References

Budding, E., Jones, K.L., Slee, O.B., Watson, L., 1999. MNRAS 305, 966.

Doiron, D.J., Mutel, R.L., 1984. AJ 89, 430.

Gagné, M. et al., 1999. ApJ 515, 423.

Güdel, M., 1997. ApJ 480, L121.

Hall, D.S., 1976. In: Fitch, W.S. (Ed.), Multiple Periodic Variable Stars (IAU Coll. 29). Reidel, Dordrecht.

Jones, K.L., Brown, A., Stewart, R.T., Slee, O.B., 1996. MNRAS 283, 1331.

Lebach, D.E., Ratner, M.I., Shapiro, I.I., Ransom, R.R., Bietenholz, M.F., Bartel, N., Lestrade, J.-F., 1999. ApJL 517, L43.

Lestrade J-F. Mutel, R.L., Preston, R.A., Phillips, R.B., 1986. In: Zeilik, M., Gibson, D.M. (Eds.), Cool Stars, Stellar Systems and the Sun. Springer Verlag, Berlin, p. 135.

Lim, J., Nelson, G.J., Castro, C., Kilkenny, D., van Wyk, F., 1992. ApJ 388, L27.

Lim, J., White, S.M., Nelson, G.J., Benz, A.O., 1994. ApJ 430, 332.

Mutel, R.L., Lestrade, J.F., Preston, R.A., Phillips, R.B., 1986. ApJ 289, 262.

Mutel, R.L., Molnar, L.A., Waltman, E.B., Ghigo, F.D., 1998. ApJ 507, 371.

Patterson, J., Caillault, J.-P., Skillman, D.R., 1993. PASP 105, 848.

Press, W.H., Flannery, B.P., Teukolsky, S.A., Vetterling, W.T., 1988. Numerical Recipes. Cambridge University Press, Cambridge.

Slee, O.B., Ables, J.G., Bachelor, R.A., Krishna-Mohan, S., Vengopal, V.R., Swarup, G., 1974. MNRAS 167, 31.

Slee, O.B., Nelson, G.J., Innis, J.L., Stewart, R.T., Vaughan, A.E., Wright, A.E., 1986. PASAu 6, 312.

Slee, O.B., Nelson, G.J., Stewart, R.T., Wright, A.E., Innis, J.L., Ryan, S.G., Vaughan, A.E., 1987. MNRAS 229, 659.

Strassmeier, K.G., Hall, D.S., Fekel, F.C., Scheck, M., 1993. A&AS 100, 173, (= 'CABS').

Trigilio, C., Umana, G., Migenes, V., 1993. MNRAS 260, 903.

Waxman, E., Kulkarni, S.R., Frail, D.A., 1998. ApJ 497, 288.